# Luminescence and photosensitivity of gadolinium labeled hematoporphyrin monomethyl ether

**Peng Wang,[1] Feng Qin,[1] Li Wang,[1] Fajun Li,[1] Yangdong Zheng,[1,4] Yunfei Song,[4] Zhiguo Zhang,[1,2,*] and Wenwu Cao[1,2,3,5]**

[1]*Condensed Matter Science and Technology Institute, Harbin Institute of Technology, Harbin 150080, China*
[2]*Laboratory of Sono- and Photo-theranostic Technologies, Harbin Institute of Technology, Harbin 150080, China*
[3]*Materials Research Institute, The Pennsylvania State University, University Park, Pennsylvania 16802, USA*
[4]*Department of Physics, Harbin Institute of Technology, 150001 Harbin, China*
[5]*dzk@psu.edu*
[*]*zhangzhiguo@hit.edu.cn*

**Abstract:** Photodynamic therapy for deep-lying lesions needs an appropriate imaging modality, precise evaluation of tissue oxygen and an effective photosensitizer. Gadolinium based metalloporphyrins Gd(III)-HMME is proposed in this study as a potential multifunctional theranostic agent, as photosensitizer, ratiometric oxygen sensor and MRI contrast agent. The time resolved spectroscopy revealed the luminescence peak of Gd(III)-HMME at 710 and 779 nm with a lifetime of 64 μs in oxygen-free methanol to be phosphorescent. This phosphorescence is strongly dependent on dissolved oxygen concentration. Its intensity in oxygen saturated methanol solution is 21% of that in deoxygenated solution. The singlet oxygen quantum yields $\Phi_{\Delta}$ of HMME and Gd(III)-HMME in air saturated methanol solution were determined to be 0.79 and 0.40 respectively using comparative spectra method. These phenomena indicate that the oxygen sensibility and production of singlet oxygen of Gd(III)-HMME can fulfill the requirement of PDT treatment.



**OCIS codes:** (160.1435) Biomaterials; (160.4760) Optical properties; (160.5690) Rare-earth-doped materials; (300.6500) Spectroscopy, time-resolved.

## References and links

1. J. P. Celli, B. Q. Spring, I. Rizvi, C. L. Evans, K. S. Samkoe, S. Verma, B. W. Pogue, and T. Hasan, "Imaging and photodynamic therapy: mechanisms, monitoring, and optimization," Chem. Rev. **110**(5), 2795–2838 (2010).
2. S. Krishnamurthy, S. K. Powers, P. Witmer, and T. Brown, "Optimal light dose for interstitial photodynamic therapy in treatment for malignant brain tumors," Lasers Surg. Med. **27**(3), 224–234 (2000).
3. A. Johansson, J. Axelsson, S. Andersson-Engels, and J. Swartling, "Realtime light dosimetry software tools for interstitial photodynamic therapy of the human prostate," Med. Phys. **34**(11), 4309–4321 (2007).
4. A. Corlu, R. Choe, T. Durduran, M. A. Rosen, M. Schweiger, S. R. Arridge, M. D. Schnall, and A. G. Yodh, "Three-dimensional in vivo fluorescence diffuse optical tomography of breast cancer in humans," Opt. Express **15**(11), 6696–6716 (2007).
5. M. T. Jarvi, M. J. Niedre, M. S. Patterson, and B. C. Wilson, "Singlet oxygen luminescence dosimetry (SOLD) for photodynamic therapy: current status, Challenges and future prospects," Photochem. Photobiol. **82**(5), 1198–1210 (2006).
6. Y. Ni, "Metalloporphyrins and functional analogues as MRI contrast agents," Curr. Med Imaging. Rev. **4**(2), 96–112 (2008).
7. M. Bottrill, L. Kwok, and N. J. Long, "Lanthanides in magnetic resonance imaging," Chem. Soc. Rev. **35**(6), 557–571 (2006).
8. H. S. He, J. P. Guo, Z. X. Zhao, W. K. Wong, W. Y. Wong, W. K. Lo, K. F. Li, L. Luo, and K. W. Cheah, "Synthesis, characterization and near-infrared photoluminescence of monoporphyrinate lanthanide complexes containing an anionic tripodal ligand," Eur. J. Inorg. Chem. **2004**(4), 837–845 (2004).
9. S. M. Borisov, G. Zenkl, and I. Klimant, "Phosphorescent platinum(II) and palladium(II) complexes with azatetrabenzoporphyrins-new red laser diode-compatible indicators for optical oxygen sensing," ACS Appl. Mater. Interfaces **2**(2), 366–374 (2010).

#201324 - $15.00 USD Received 14 Nov 2013; revised 27 Dec 2013; accepted 29 Dec 2013; published 28 Jan 2014

10. K. Koren, S. M. Borisov, R. Saf, and I. Klimant, "Strongly phosphorescent iridium(III)-porphyrins new oxygen indicators with tunable photophysical properties and functionalities," Eur. J. Inorg. Chem. **2011**(10), 1531–1534 (2011).
11. P. Mroz, J. Bhaumik, D. K. Dogutan, Z. Aly, Z. Kamal, L. Khalid, H. L. Kee, D. F. Bocian, D. Holten, J. S. Lindsey, and M. R. Hamblin, "Imidazole metalloporphyrins as photosensitizers for photodynamic therapy: role of molecular charge, central metal and hydroxyl radical production," Cancer Lett. **282**(1), 63–76 (2009).
12. H. J. Vreman and D. K. Stevenson, "Metalloporphyrin-enhanced photodegradation of bilirubin in vitro," Am. J. Dis. Child. **144**(5), 590–594 (1990).
13. S. D. Appleton, M. L. Chretien, B. E. McLaughlin, H. J. Vreman, D. K. Stevenson, J. F. Brien, K. Nakatsu, D. H. Maurice, and G. S. Marks, "Selective inhibition of heme oxygenase, without inhibition of nitric oxide synthase or soluble guanylyl cyclase, by metalloporphyrins at low concentrations," Drug Metab. Dispos. **27**(10), 1214–1219 (1999).
14. M. A. Oar, W. R. Dichtel, J. M. Serin, J. M. J. Frechet, J. E. Rogers, J. E. Slagle, P. A. Fleitz, L. S. Tan, T. Y. Ohulchanskyy, and P. N. Prasad, "Light-harvesting chromophores with metalated porphyrin cores for tuned photosensitization of singlet oxygen via two-photon excited FRET," Chem. Mater. **18**(16), 3682–3692 (2006).
15. C. Brushett, B. Qiu, E. Atalar, and X. Yang, "High-resolution MRI of deep-seated atherosclerotic arteries using motexafin gadolinium," J. Magn. Reson. Imaging **27**(1), 246–250 (2008).
16. Y. Ni, C. Pislaru, H. Bosmans, S. Pislaru, Y. Miao, F. Van de Werf, W. Semmler, and G. Marchal, "Validation of intracoronary delivery of metalloporphyrin as an in vivo "histochemical staining" for myocardial infarction with MR imaging," Acad. Radiol. **5**(Suppl 1), S37–S41, discussion S45–S46 (1998).
17. V. M. Runge, B. R. Carollo, C. R. Wolf, K. L. Nelson, and D. Y. Gelblum, "Gd DTPA: a review of clinical indications in central nervous system magnetic resonance imaging," Radiographics **9**(5), 929–958 (1989).
18. A. M. Evens, "Motexafin gadolinium: a redox-active tumor selective agent for the treatment of cancer," Curr. Opin. Oncol. **16**(6), 576–580 (2004).
19. A. Harriman, "Luminescence of porphyrins and metalloporphyrins. Part 3. -Heavy-atom effects," J. Chem. Soc., Faraday Trans. II **77**(7), 1281–1291 (1981).
20. E. G. Ermolina, R. T. Kuznetsova, T. A. Solodova, E. N. Telminov, T. N. Kopylova, G. V. Mayer, N. N. Semenishyn, N. V. Rusakova, and Y. V. Korovin, "Photophysics and oxygen sensing properties of tetraphenylporphyrin lanthanide complexes," Dyes Pigments **97**(1), 209–214 (2013).
21. J. Cheng, H. Liang, Q. Li, C. Peng, Z. Li, S. Shi, L. Yang, Z. Tian, Y. Tian, Z. Zhang, and W. Cao, "Hematoporphyrin monomethyl ether-mediated photodynamic effects on THP-1 cell-derived macrophages," J. Photochem. Photobiol. B **101**(1), 9–15 (2010).
22. T. S. Srivastava, "Lanthanide octaethylprophyrins: preparation, association, and interaction with axial ligands," Bioinorg. Chem. **8**(1), 61–76 (1978).
23. A. Ogunsipe and T. Nyokong, "Photophysical and photochemical studies of sulphonated non-transition metal phthalocyanines in aqueous and non-aqueous media," J. Photochem. Photobiol. Chem. **173**(2), 211–220 (2005).
24. S. Mathai, T. A. Smith, and K. P. Ghiggino, "Singlet oxygen quantum yields of potential porphyrin-based photosensitisers for photodynamic therapy," Photochem. Photobiol. Sci. **6**(9), 995–1002 (2007).
25. H. Ryeng and A. Ghosh, "Do nonplanar distortions of porphyrins bring about strongly red-shifted electronic spectra? Controversy, consensus, new developments, and relevance to chelatases," J. Am. Chem. Soc. **124**(27), 8099–8103 (2002).
26. M. Gouterman, "Optical spectra and electronic structure of porphyrins and related rings," in *The Porphyrins*, Part 3A(Academic Press, 1978).
27. T. C. Lei, G. F. Glazner, M. Duffy, L. Scherrer, S. Pendyala, B. Li, X. L. Wang, H. W. Wang, and Z. Huang, "Optical properties of hematoporphyrin monomethyl ether (HMME), a PDT photosensitizer," Photodiagn. Photodyn. Ther. **9**(3), 232–242 (2012).
28. R. Battino, T. R. Rettich, and T. Tominaga, "The solubility of oxygen and ozone in liquids," J. Phys. Chem. Ref. Data **12**(2), 163–178 (1983).

## 1. Introduction

Photodynamic therapy (PDT) and fluorescence imaging has long been used for treatment and diagnosis of superficial cancer. PDT requires photosensitizer (PS), light and molecular oxygen. When PSs are exposed to light of appropriate wavelength, they produce highly cytotoxic singlet oxygen ($^1O_2$) to destruct the diseased tissue and the fluorescence could be used for diagnosis and image guided resection [1]. PDT is minimally invasive, has few side effects, rapid recovery from the treatment and could be operated repeatedly. However clinical applications of PDT treatment are restricted by the limited penetration of light. In recent years, interstitial PDT has been studied for treatment of larger and deeper lesions [2, 3]. This treatment approach needs images to provide the morphological and physiological information of the diseased tissues. MRI guided diffuse optical spectroscopy (DOS) and fluorescence tomography imaging (FTI) [4] have been developed for diagnosis of tumors. With these technologies, the three-dimensional (3D) dosimetric planning of interstitial PDT can be realized. Another problem for interstitial PDT is to estimate the efficacy of PDT. Singlet

#201324 - $15.00 USD Received 14 Nov 2013; revised 27 Dec 2013; accepted 29 Dec 2013; published 28 Jan 2014

oxygen luminescence dosimetry is the golden standard. However its clinical applications are limited due to its very low luminescence intensity [5]. The treatment planning must consider the three elements of PDT, not only light. Therefore, interstitial PDT would benefit from these multimodality methods with the theranostic agents that could function as MRI contrast agent (CA), photosensitizer and oxygen indicator at the same time.

Porphyrins are the most popular PSs for their tumor selective uptake, strong fluorescence emission and photosensitizing effects. However, metalloporphyrins are better choice as multifunctional theranostic agent due to their diverse properties. In the biomedical field, metalloporphyrins have been studied for MRI contrast agents [6, 7], near-infrared probe [8], oxygen sensor [9, 10], photodynamic therapy [11], photodegradation of bilirubin [12], inhibitors of heme oxygenase [13], etc. The physiochemical nature of metalloporphyrins differs by the central metal ion in the molecule. For example, the diamagnetic metalloporphyrins have longer triplet lifetime and better photosensitivity in some circumstances [14]; the platinum metalloporphyrins have been developed for oxygen sensing both in air and in solutions; the paramagnetic metalloporphyrins have been used as MRI CAs, etc. In pharmacokinetics, metalloporphyrins are reported to be necrosis-avid rather than tumor-avid, which means that metalloporphyrins based photosensitizers are only suitable for malignant tumors because in premalignant cancer, there are very few necrotic cells. This property enables metalloporphyrins to find applications in atherosclerotic plaque imaging [15], myocardial infarction delineation [16], etc. To fulfill the requirements of diagnosis and PDT treatments, the selection of appropriate central metal ion and porphyrin matrix is critically important.

Trivalent gadolinium ion Gd(III) has an electronic configuration of $[Xe]4f^7$, resulting in a high degree of paramagnetism. Therefore, gadolinium metalated porphyrins and associated complexes have long been used as MRI CAs, including Gd-DTPA [17] and Motexafin gadolinium [18]. The strong paramagnetism, heavy-atom effect [19] and special energy levels in which the lowest energy level of Gd(III) is above the singlet ($S_1$ and $S_2$) and triplet ($T_1$) of porphyrins, indicate gadolinium porphyrins having relatively high quantum yields of triplet state $\Phi_T$. Two important physiochemical properties (phosphorescence and photosensitivity) are strongly relevant with generation of triple states and oxygen concentration. Generally, the phosphorescence intensity decreases with oxygen concentration in accordance with Stern-Volmer relationship. The phosphorescence of gadolinium porphyrins has been observed and used in optical oxygen sensing fibers or thin films [20]. Here we infer that the $\Phi_\Delta$ would increase with the increase of dissolved oxygen concentration. For biomedical applications, attentions should be also paid to the solubility, cell permeability and pharmacokinetics which are strongly relevant with the porphyrins matrix. Hematoporphyrin monomethyl ether is a second generation photosensitizer and has been used in clinical therapy of many diseases. The chemical structure of HMME offers a balance between hydrophilic and hydrophobic, therefore has excellent cell permeability [21], which would be a good choice of molecular matrix for cell-penetrating drug.

In this study, gadolinium metalated hematoporphyrin methyl ether Gd(III)-HMME was synthesized and characterized with mass spectra and UV-visible spectra. Both the molecular weight and the electronic structure confirmed the successful synthesis of the metalloporphyrins. The weak fluorescence and strong room temperature phosphorescence were observed and proved with time resolved spectroscopy. The dependence of the luminescence spectra of Gd(III)-HMME on dissolved oxygen levels was determined, which shows that the fluorescence intensity is independent of oxygen levels while the phosphorescence is strongly dependent on oxygen level. The phosphorescence intensity decreased by 79% in oxygen saturated methanol. This phenomenon indicates the potential of Gd(III)-HMME to be an optical ratiometric oxygen indicator. The singlet oxygen quantum yields $\Phi_\Delta$ of Gd(III)-HMME and HMME were determined with a comparative method based on spectrophotometer using 1,3-diphenylisobenzofuran (DPBF) as singlet oxygen capture and 4,5,6,7,-tetrachloro-2',4',5′,7'-tetraiodofluorescein disodium salt (Rose Bengal) as a reference. Although the $\Phi_\Delta$ of Gd(III)-HMME is only half of that of HMME, the efficiency of

#201324 - $15.00 USD Received 14 Nov 2013; revised 27 Dec 2013; accepted 29 Dec 2013; published 28 Jan 2014

photosensitization is high enough for the PDT purpose. The synergistic effect of oxygen sensing capability, photosensitivity, MRI enhancement, cell permeability and the necrosis affinity would give Gd(III)-HMME a wide potential application prospect.

## 2. Experimental

### *2.1 Chemicals*

Anhydrous gadolinium(III) chloride ($GdCl_3$), 1,3-diphenylisobenzofuran (DPBF) and 4,5,6,7,-tetrachloro-2',4',5′,7'-tetraiodofluorescein disodium salt (Rose Bengal) were obtained from J&K Scientific Ltd. Hematoporphyrin monomethyl ether (HMME) was purchased from Shanghai Xianhui Pharmacuetical Co. Ltd. All chemical reagents were analytical reagent grade and used without further purification.

Gd(III)-HMME was synthesized in imidazole at high temperature with gentle argon flow protection based on T. S. Srivastava's method [22]. 5 g imidazole, 12 mg HMME and 150 mg anhydrous $GdCl_3$ were added into a 50 ml round bottom flask with argon flow protection for 30 min. Then, the mixture was heated and kept at 220 °C and stirred magnetically for 2 h protected with gentle argon flow. After cooling down to room temperature, the mixture was dissolved in 10 ml methanol and dialyzed (cutoff size = 800) against methanol for 5 times.

### *2.2 Instrumentation*

Mass spectroscopy were recorded by liquid chromatography/mass spectra (LC/MS) analyzing system (Thermo Finnigan Surveyor LCQ DECA XP plus, USA). UV-visible absorption spectra were determined with miniature fiber optic spectrometer QE65000 (Ocean Optics, USA) equipped with the deuterium lamp. 532 nm solid laser (CLO Laser DPGL-500L, China) was used for excitation of photosensitizers. Laser power meter (Ophir Photonics Group, Israel) was used to determine the output power of the 532 nm laser. In the time resolved spectroscopy measurements, the laser pulses of 100 fs at 800 nm from Ti: sapphire femtosecond laser (Spectra-Physics, USA) passed through a double-frequency BBO crystal. The output pulses at 400 nm were used for the luminescence excitation of HMME and Gd(III)-HMME. The luminescence spectra were recorded every 2 ns with the spectrometer (Bruker Optics) and intensified charge coupled device (ICCD, IStar740, CCI010, Andor), which was trigged by synchronization and delay generator (SDG, Spectra-Physics, USA) and Digital Delay/Pulse Generator (Stanford Research Systems).

### *2.3 Oxygen sensitivity of luminescence spectra*

The luminescence spectra in solutions with different dissolved oxygen concentrations were recorded. The oxygen and nitrogen flows were controlled with two gas mass flow meters and mixed in a bottle. The gas mixture was loaded into Gd(III)-HMME methanol solution with a needle and then kept above the solution surface. The dissolved oxygen level was then controlled by the ratio of flow rates of oxygen and nitrogen. The proportion of oxygen was set as 3%, 12.7%, 22.4% and 100%. A vacuum pump was used to get the solution deoxygenated. Optics fiber loading light at 405 nm was used for excitation and the luminescence spectra were measured using a miniature spectrometer QE65000.

### *2.4 Singlet oxygen production*

In this study, $\Phi_\Delta$ of HMME and Gd-HMME in air saturated methanol at room temperature were determined by a spectrophotometric method. In this relative method, there are two critical analytical reagents, singlet oxygen capture with typical absorption or fluorescence spectra and photosensitizer with well determined $\Phi_\Delta$. At least three data are used in this analysis. They are: $\Phi_\Delta$ of the photosensitizer of the reference reagent, the absorption of excitation light and the photodegradation rates of singlet oxygen capture in each mixture solutions with different photosensitizers. The $\Phi_\Delta$ is determined based on Eq. (1).

#201324 - $15.00 USD Received 14 Nov 2013; revised 27 Dec 2013; accepted 29 Dec 2013; published 28 Jan 2014

$$\frac{\Phi_{\Delta} I_{abs}}{k} = \frac{\Phi_{\Delta}^{ref} I_{abs}^{ref}}{k^{ref}}, \tag{1}$$

where $k$ is the degradation rate of the singlet oxygen capture DPBF, mainly induced by the reaction with singlet oxygen; the superscript ref stands for the reference reagent Rose Bengal; $I_{abs}$ represents the absorption of excitation light by photosensitizer [23]. $I_{abs}$ is determined by concentrations of photosensitizers, extinction coefficients and incident light intensities as described by Eq. (2).

$$I_{abs} = \int I_{532}(\lambda) \times \left(1 - e^{-\varepsilon(\lambda) NL}\right) d\lambda, \tag{2}$$

where $I_{532}(\lambda)$ is the emission spectra of the 532 nm laser, $\varepsilon(\lambda)$ is the extinction spectra of each photosensitizer, $N$ represents the concentration of that photosensitizer and $L$ represents the is the light path in the cuvette.

Rose Bengal was used as the reference reagent $\Phi_{\Delta}^{RB} = 0.76$ in air saturated methanol solution at room temperature [24]. DPBF is a highly singlet oxygen selective indicator. DPBF has strong absorption at 415 nm and the product of chemical reaction between DPBF and singlet oxygen has no absorption in this range. The UV-visible absorption spectra in the range of 400 nm to 430 nm were uesd to monitor the photostability of DPBF under irradiation at 532 nm and the photodegradation in mixtures with photosensitizers. Four samples were prepared: (1) DPBF 30 μM; (2) DPBF 30 μM, Rose Bengal 1 μM; (3) DPBF 30 μM, HMME 2 μM; (4) DPBF 30 μM, Gd-HMME 2 μM. Each sample of 3 ml was put in silica curette of 1 cm length and illuminated with 532 nm laser at the same power density of 1 mW/cm$^2$, corresponding to a photon density of 1.3 × 10$^{13}$/cm$^3$. The decrease of DPBF was monitored with UV-visible absorption spectroscopy simultaneously. The absorption spectra of DPBF were recorded every 3 min and the degradation rate of DPBF $k$ was determined accordingly. In this experiment, all measurements were taken at room temperature under 1 atm.

## 3. Results and discussion

### *3.1 Synthesis and characterization*

Figure 1 presents the chemical structures of HMME and Gd(III)-HMME, and the chloride ion is omitted in the figure. The ESI mass spectrum of Gd(III)-HMME has an intense peak at m/z = 803.05 (calc m/z = 803.17) corresponding to [Cl-Gd(III)-HMME + H$^+$] as shown in Fig. 2.

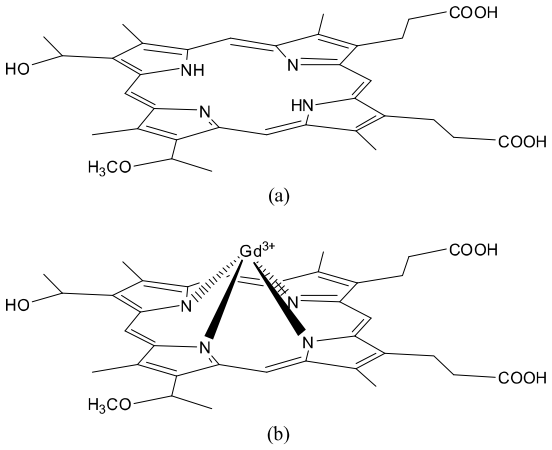


Fig. 1. Chemical structures of (a) HMME and (b) Gd(III)-HMME.

The UV-visible absorption spectra and luminescence spectra of HMME and Gd(III)-HMME are presented in Fig. 3. The gadolinium ion has a relatively large ionic radius of 93.8

#201324 - $15.00 USD Received 14 Nov 2013; revised 27 Dec 2013; accepted 29 Dec 2013; published 28 Jan 2014

pm and its corresponding metalloporphyrins have an out-of-plane structure [25]. The out- of-plane results in red shift of Q-band absorption peaks. The change of symmetry from $D_{2h}$ to $C_{4v}$ leads to the Q-band peak reduction. The Q-band peaks of HMME are at 499 nm, 530 nm, 568 nm and 624 nm [26, 27]. The Q-band peaks of Gd(III)-HMME are at 538 nm and 571 nm. The fluorescence intensity of Gd(III)-HMME decreased significantly and their peaks are in the mirror positions of the absorption spectra, in accordance with Franck-Condon principle. In addition, Gd(III)-HMME also exhibits strong room temperature luminescence emission and the peaks are at 712 nm and 780 nm.

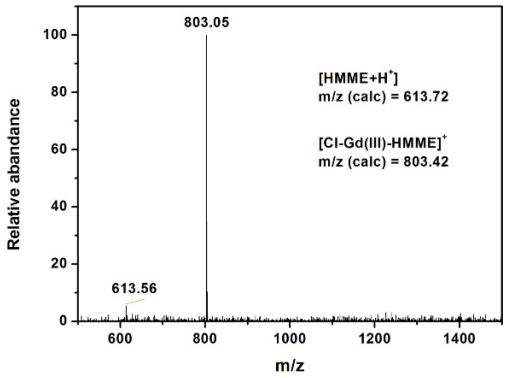


Fig. 2. Mass spectrum of Gd(III)-HMME (Positive ion ESI source). [HMME + $H^+$]: HMME molecule attached with a proton; [Cl-Gd(III)-HMME]$^+$: Gd(III)-HMME molecule attached with one chloride ion.

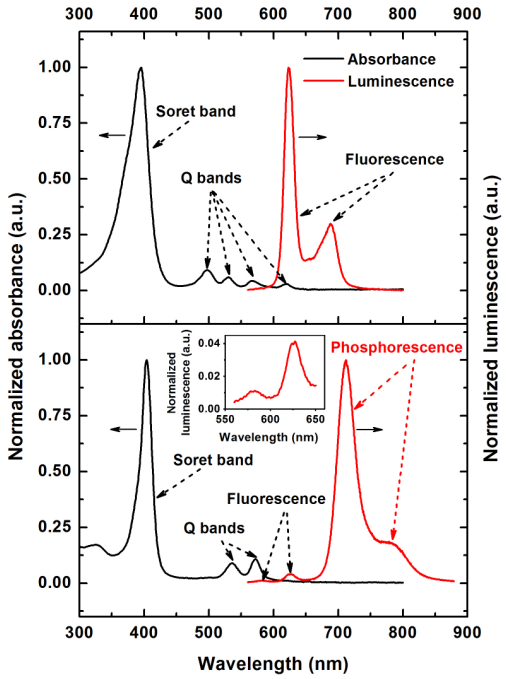


Fig. 3. Normalized absorption spectra (black solid line) of HMME and Gd(III)-HMME and the corresponding luminescence spectra (red solid line) in oxygen-free methanol solutions. The Soret bands and Q bands are labeled. The fluorescence emissions are labeled. Inset figure shows the weak fluorescence emission of Gd(III)-HMME. The strong room-temperature redshift luminescence emissions are marked as phosphorescence.

#201324 - $15.00 USD Received 14 Nov 2013; revised 27 Dec 2013; accepted 29 Dec 2013; published 28 Jan 2014

*3.2 Luminescence lifetimes of Gd(III)-HMME and HMME*

Figure 4(a) presents the luminescence decay curves of HMME and Gd(III)-HMME in air-saturated methanol solutions at 625 nm, respectively. The fluorescence lifetime of Gd(III)-HMME is smaller than that of HMME. Figure 4(b) shows the luminescence decay curves of Gd(III)-HMME in deaerated methanol. The lifetime of 51 μs indicates that the emission is from the triplet energy level. The electron configuration of trivalent gadolinium ion is $[Xe]4f^7$. The heavy atom effect and the paramagnetism enhanced the singlet-triplet intersystem crossing [19]. This effect reduces the fluorescence intensity and makes strong phosphorescence possible. In contrast to $Yb^{3+}$, $Er^{3+}$ and $Nd^{3+}$ [6], which have lower energy levels to the single states ($S_1$ and $S_2$) and triple states ($T_1$) of porphyrins, $Gd^{3+}$ ion cannot receive energy by means of the Förster resonance energy transfer. For these reasons, gadolinium porphyrins have very strong room temperature phosphorescent emission.

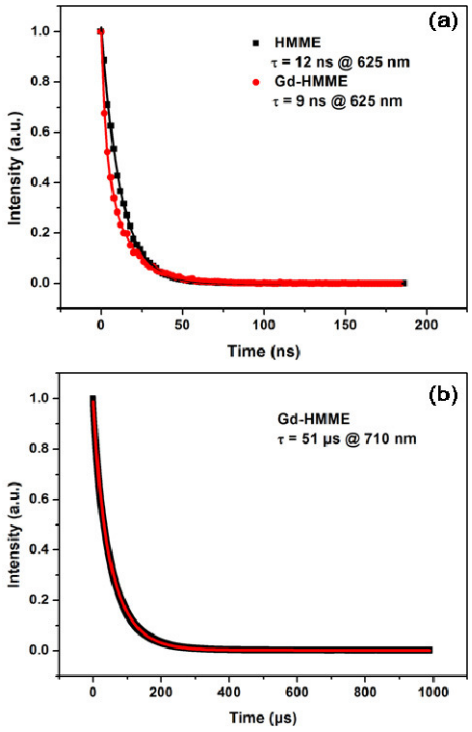


Fig. 4. The decay curves of the fluorescence emission of HMME and Gd(III)-HMME at 625 nm in methanol solution (a) and the decay curve luminescence emission of Gd(III)-HMME at 710 nm in oxygen-free methanol solution (b).

*3.3 Oxygen dependence*

The relationship between the luminescence intensity of Gd(III)-HMME and dissolved oxygen concentration was studied. Figure 5 presents the luminescence spectra in methanol with different dissolved oxygen concentrations. The fluorescence intensities at 625 nm kept the same and the phosphorescence intensities at 710 nm depended strongly on dissolved oxygen concentrations and decreased by 79% in oxygen saturated methanol solution. The phosphorescence emission intensity and lifetime always comply with the Stern-Volmer relationship and the fluorescence offers an invariant referent. Therefore, the ratio between phosphorescence and fluorescence could be used for oxygen indication after calibration.

#201324 - $15.00 USD Received 14 Nov 2013; revised 27 Dec 2013; accepted 29 Dec 2013; published 28 Jan 2014

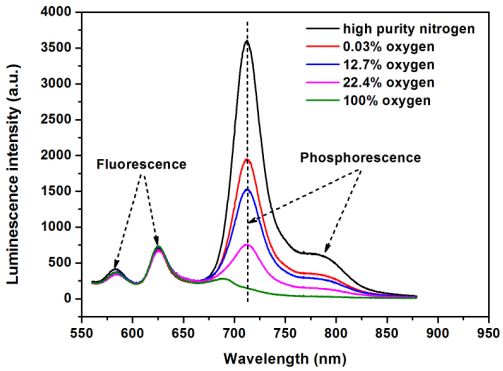


Fig. 5. The luminescence spectra of Gd(III)-HMME in methanol solutions with different dissolved oxygen concentrations. The fluorescence and phosphorescence peaks are labeled respectively.

### *3.4 Singlet oxygen production*

Singlet oxygen production is one of the most important photochemical properties of photosensitizers and its $\Phi_\Delta$ is an important parameter for the PDT dosimetry calculation. The generation of singlet oxygen is related with the generation of quantum yield of triplet $\Phi_T$ of metalloporphyrins and the energy transfer from the triplet state to ground state oxygen molecule. Therefore, $\Phi_\Delta$ is affected not only by inner conversion, intersystem crossing, which differs from the type of solvent, temperature and pressure, but also by the concentrations of oxygen molecules. In air saturated methanol solution, the concentration of dissolved oxygen is 1.99 ± 0.18 mM [28], which molar concentration is hundreds of times larger than that of DPBF. In other word, the oxygen level in solutions used in this study could be considered as constants.

Figure 6 shows the absorption spectra DPBF in methanol solution by itself and in the mixture solution of Rose Bengal, HMME and Gd(III)-HMME, respectively. The photostability of DPBF is excellent under the light excitation at 532 nm. The residual concentration of DPBF and the excitation time follows exponential relationship in solutions with photosensitizers.

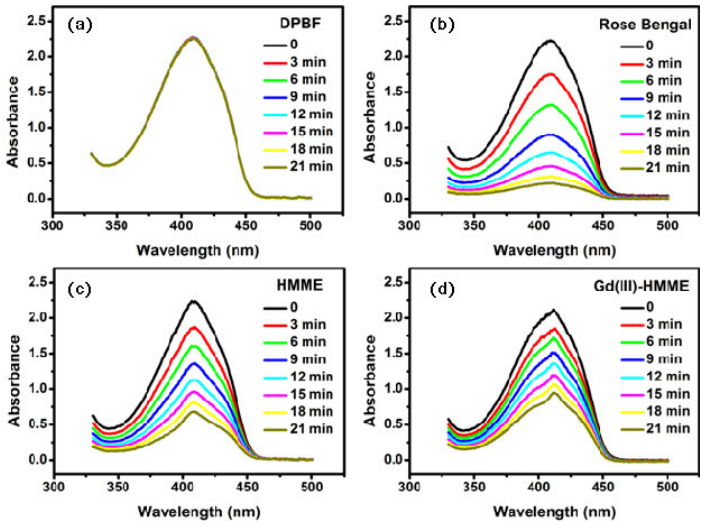


Fig. 6. The absorption spectra of DPBF in methanol solutions with (a) no photosensitizer (b) 1 μM Rose Bengal (c) 2 μM HMME (d) 2 μM Gd(III)-HMME with 532 nm laser illumination and recorded every 3 min.

#201324 - $15.00 USD Received 14 Nov 2013; revised 27 Dec 2013; accepted 29 Dec 2013; published 28 Jan 2014

Figure 7 shows the time dependence of relative consumption of DPBF in four circumstances. The concentrations of DPBF are determined with the absorption spectra shown in Fig. 6. The degradation rates of DPBF are determined by linear fitting. The degradation rates of DPBF, the absorption of excitation light at 532 nm and $\Phi_\Delta$ calculated according to Eq. (1) are presented in Table 1. Although the singlet oxygen quantum yield of Gd(III)-HMME ($\Phi_\Delta$ = 0.40) is only about one half of that of HMME ($\Phi_\Delta$ = 0.79) in air-saturated methanol solution at room temperature, the singlet oxygen generation is still more than sufficient for PDT purpose.

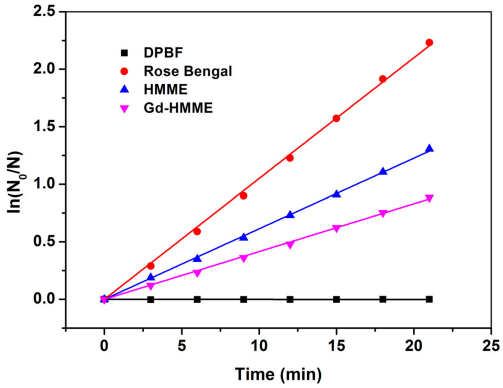


Fig. 7. Relative consumptions of DPBF under irradiation mixed with different photosensitizers and recorded every 3 min.

**Table 1. Chemicals, concentrations and calculated degradation rates $k$, absorption $I_{abs}$ and sensitization efficiencies $\Phi_\Delta$.**

| Photosensitizers | Concentrations [μM] | $k$ [$s^{-1}$] | $I_{abs}$ | $\Phi_\Delta$ |
|---|---|---|---|---|
| Rose Bengal | 1 | 0.100 | 3.04 | 0.76* |
| HMME | 2 | 0.061 | 1.79 | 0.79 |
| Gd-HMME | 2 | 0.041 | 2.36 | 0.40 |

*Date from ref [23].

## 4. Conclusion

In conclusion, gadolinium porphyrin Gd(III)-HMME was synthesized and characterized with UV-visible spectra and mass spectra. The photophysical and photochemical properties were studied with spectral methods. Strong room-temperature phosphorescence was observed and further proved by time resolved spectroscopy analysis. The fluorescence intensity of Gd(III)-HMME is insensitive to dissolved oxygen concentration but its phosphorescence shows strong dependence on dissolved oxygen levels. This phenomenon makes Gd(III)-HMME a promising and potential ratiometric oxygen sensor. Although $\Phi_\Delta$ of Gd(III)-HMME is 0.4 in air saturated methanol solution at room temperature, only about half of that of Rose Bengal or HMME, the photosensitivity of Gd(III)-HMME is still relatively strong among metalloporphyrins. The inherent paramagnetism of $Gd^{3+}$ and the physiochemical properties will help Gd(III)-HMME find various applications, especially for biomedical purposes like MRI-guided PDT treatment.

## Acknowledgments

This work was financially supported by the National Key Basic Research Program of China (973 Program) under Grant No. 2013CB632900.

#201324 - $15.00 USD Received 14 Nov 2013; revised 27 Dec 2013; accepted 29 Dec 2013; published 28 Jan 2014